# Predicting the entrainment of reentrant cardiac waves using phase resetting curves

Leon Glass,[1] Yoshihiko Nagai,[1] Kevin Hall,[2] Mario Talajic,[3] and Stanley Nattel[3]
[1]*Centre for Nonlinear Dynamics and Department of Physiology, McGill University, 3655 Promenade Sir William Osler, Montreal, Quebec, Canada H3G 1Y6*
[2]*Entelos Inc., 4040 Campbell Avenue, Suite 200, Menlo Park, California 94040*
[3]*Montreal Heart Institute, Montreal, Quebec, Canada H1T 1C8*
(Received 14 June 2001; revised manuscript received 4 September 2001; published 24 January 2002)

Excitable media, such as the Belousov-Zhabotinsky medium or the heart, are capable of supporting excitation waves that circulate in a closed repetitive path—a phenomenon known as reentrant excitation. A single stimulus, depending on its magnitude, timing, and location, can cause a time shift of the reentrant excitation called resetting. The present study examines the ability of resetting data to predict the effects of periodic stimuli on reentrant excitation circulating on an annular domain. We compare the results of the theoretical models with experiments carried out in an animal model of a dangerous reentrant cardiac rhythm. The current work may lead to improved approaches to therapy through a better understanding of how typical clinical stimuli interact with abnormal reentrant cardiac rhythms.

DOI: 10.1103/PhysRevE.65.021908 PACS number(s): 87.19.−j, 05.45.−a, 05.40.−a, 89.75.−k

## I. INTRODUCTION

The abnormal rhythms of the human heart are a focus of research not only because of their relevance to human health, but also because of the significant mathematical and physical concepts raised by their dynamics. The heart is an example of an excitable medium characterized by the following two properties [1–4]: (1) a small but finite perturbation away from a steady state will lead to a large excursion (an excitation or an *action potential*) before the steady state is reestablished; (2) following the onset of the excitation, there is an interval during which a perturbation does not induce a new excitation. The interval is called the *refractory period*. A consequence of the refractory period is that colliding waves annihilate each other. Since the Belousov-Zhabotinsky chemical reaction is also an example of an excitable medium, many phenomena similar to those in the heart can be observed in chemical media [5,6].

The current work was motivated by the need to develop an appropriate mathematical framework for procedures used by physicians to diagnose and treat cardiac arrhythmias [7]. During clinical cardiac electrophysiological procedures, cardiologists insert several catheters directly into the heart. Usually, the catheters are first placed in veins, and then are pushed through the veins to a suitable target in the heart. The catheters are used to carry out three different procedures: (i) to record electrical activity in the heart; (ii) to deliver electrical stimuli (usually either a single stimulus or a periodic train of stimuli) directly to the heart; and (iii) to ablate localized regions of the heart by delivering radiofrequency radiation to burn and kill cells in localized regions. The anatomical basis for the ablation procedure derives from a conceptual model of reentrant arrhythmias that assumes there is a ringlike or annular domain that supports the circulating wave [8–17]. If the ablation succeeds in cutting the ring or annulus, then the substrate for the arrhythmia is destroyed and the patient is cured.

Previous work has analyzed the dynamics induced by a single stimulus delivered to homogeneously oscillating systems [18,19] and oscillations in spatially dispersed systems showing reentrant excitation [20–24]. A single stimulus, depending on its magnitude, timing, and location, can cause a time shift of the endogenous rhythm. The time shift is called resetting, and for stimuli delivered to a homogeneous system or an excitation circulating in a ring, the resetting data can be used to predict the effects of periodic stimuli [18–20]. An important exception to the predictive power of resetting data occurs when a stimulus is too distant from a reentrant circuit to cause resetting. However, periodic stimulation at such a site can entrain the reentrant rhythm [5,25]. Our goal in what follows is to carefully examine the conditions under which resetting data fail to predict the effects of periodic stimuli delivered to reentrant excitation circulating around an annulus. We show that discrepancies between the predicted results and the observations may give additional information about the location of the stimulating and recording sites relative to the reentrant circuit. In Sec. II we present the mathematical background. We study the effects of single and periodic stimuli in a simple model of conduction in Sec. III and in a nonlinear partial differential equation model of excitable media in Sec. IV. An experimental example is given in Sec. V.

## II. MATHEMATICAL FORMALISM

Earlier theoretical work showed that knowledge of the resetting induced by a brief stimulus delivered at different phases of limit cycle in an ordinary differential equation can be used to predict the effects of periodic stimulation, provided the limit cycle is rapidly reestablished following the stimulus, and the stimulus does not change the properties of the nonlinear equation [18,19]. Application of the theoretical methods to study the effects of periodic stimulation of spontaneously beating aggregates of heart cells gives good agreement between theory and experiment. The same theory was capable of predicting the effects of periodic stimulation of a pulse circulating on a one-dimensional ring based on the resetting induced by a single stimulus located directly on the ring [20]. We now extend the theory to the case in which the

 

oscillation is associated with a wave circulating on an annulus with stimulating and measuring probes in arbitrary locations.

### A. Global phase and *W* isochrons

Assume a dynamical system with a stable limit cycle $\gamma$ with period $T_0$. In the current case, we consider a stably circulating wave of excitation that is described by some appropriate nonlinear partial differential equation. An arbitrary point in function state space $y(\mathbf{r},t)$ gives the values of all the variables in physical space $\mathbf{r}$ at a given time $t$. The coordinates of the wave front are defined by a locus of points in the physical space satisfying $\xi(\mathbf{r},t)=0$, where $\xi$ is an appropriate function to localize the wave front. We arbitrarily set the time coordinate so that the excitation wave front is in some fiducial position when $t=0$. We take $\mathbf{r}^*$ to be an arbitrary point on the wave front when $t=0$, so that $\mathbf{r}^* \in \xi(\mathbf{r},0)$. For times $t>0$ the global phase of the system is given by $\Phi = t/T_0 \pmod 1$.

The *basin of attraction* of $\gamma$ corresponds to all states in function state space that approach $\gamma$ in the limit $t\to\infty$. Let $x(t=0)$ and $x'(t=0)$ be the initial conditions of a state on the cycle and a state not on the cycle, respectively, and $x(t),x'(t)$ be the coordinates of the trajectories at time $t$ [26]. If $\lim d[x(t),x'(t)]=0$, where $d[\cdot]$ represents an appropriate metric defined on the solution space, as $t\to\infty$, then the latent phase of $x'(0)$ is the same as the phase of $x(0)$. The union of all functions with the same latent phase constitutes the *W* isochron [27–29].

### B. Local phase and resetting

In the cardiological context, a probe is inserted into the heart. This probe measures activity at a given location in the heart. Since the excitation wave is spreading in the heart, the excitation wave front will reach different regions of the heart at different times.

In this experimental context it is useful to define the local phase $\phi(\mathbf{r},t)$ measured at position $\mathbf{r}$ and time $t$. $\phi(\mathbf{r},t)$ is the time duration since the previous activation normalized by the period of the rhythm $T_0$,

$$\phi(\mathbf{r},t)=\frac{t-\tau(\mathbf{r})}{T_0} \pmod 1, \tag{1}$$

where $\tau(\mathbf{r})$ is the last time before $t$ that the point $\mathbf{r}$ was excited. The phase difference at locations $\mathbf{r}_1$ and $\mathbf{r}_2$ is determined by the time delay between the activation of probes at the different locations:

$$\phi(\mathbf{r}_1,t)-\phi(\mathbf{r}_2,t)=-\frac{\Delta t_{12}}{T_0}, \tag{2}$$

where $\Delta t_{12}=\tau(\mathbf{r}_1)-\tau(\mathbf{r}_2)$ is the time difference between the activation of probes $p_1$ and $p_2$.

The global phase and the local phase are related by the expression

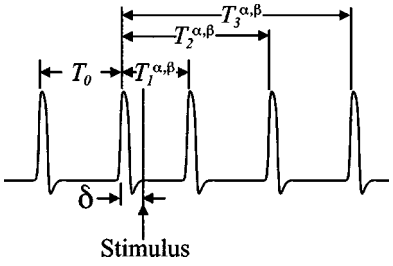


FIG. 1. Definition of measurements to construct the resetting curve from a stimulation delivered at location $\alpha$, with recording at location $\beta$. The intrinsic period of the reentrant wave is $T_0$. $\delta$ is the time interval from the last complex before the stimulus to the stimulus. $T_j^{\alpha,\beta}$ is the time from the last complex before the stimulus to the $j$th complex after the stimulus.

$$\phi(\mathbf{r},t)=\Phi(t)-\frac{\tau(\mathbf{r})-\tau(\mathbf{r}^*)}{T_0}. \tag{3}$$

Following a single perturbation of relatively short duration delivered to the system, the oscillation may be reestablished with the same period as before, but with altered timing of subsequent oscillations. This shift in the timing of the oscillation is called *phase resetting* or simply resetting.

In systems distributed in space, the effects of a stimulus depend not only on its magnitude and timing, but also on its location. The effect of a stimulus is determined by measuring the activation times since the activation prior to the stimulus $T_1^{\alpha,\beta}, T_2^{\alpha,\beta},\ldots,T_k^{\alpha,\beta}$ where the superscript $\alpha$ represents the position of the stimulus, the superscript $\beta$ indicates the position at which the phase is being measured, and the subscript $k$ indicates the number of activations since the stimulus was delivered (Fig. 1) [23,24]. If there is no resetting, we have $T_j^{\alpha,\beta}(\Phi)=jT_0$. If there is resetting, then $T_j^{\alpha,\beta}(\Phi) - T_{j-1}^{\alpha,\beta}(\Phi)$ should converge to $T_0$ for sufficiently large $j$ since we assume that the reentrant rhythm is stable.

If measurements of resetting are carried out at two different locations $\mathbf{r}_1$ and $\mathbf{r}_2$ due to a single stimulus at $\alpha$, then using Eq. (2) the measured resetting curves are related to each other by [24]

$$T_j^{\alpha,\mathbf{r}_1}(\phi(\mathbf{r}_1,t))=T_j^{\alpha,\mathbf{r}_1}\left(\phi(\mathbf{r}_2,t)-\frac{\Delta t_{12}}{T_0}\right), \tag{4}$$

for $j$ large enough that transient effects of the stimulus have dissipated.

### C. Entrainment

The effect of a perturbation delivered during the course of the cycle is to shift the state off $x\in\gamma$ on one *W* isochron $W^s(x)$ to a *perturbed state*. If the perturbed state is in the basin of attraction of $\gamma$, the effects of the perturbation can be represented by a phase transition curve $g(\Phi)$, where $\Phi$ is the global phase of the initial state $x$ at which the stimulus is presented, and $g(\Phi)$ is the asymptotic global phase at the termination of the stimulus. The phase transition curve $g(\Phi)$ is not defined for those stimuli that lead to shifting an oscillation outside its basin of attraction.

The phase transition curve can be determined from the phase resetting curve [18–20]. First assume the measuring probe is placed at a locus $\mathbf{r}^*$ that is excited when the global phase $\Phi=0$. We find

$$g(\Phi)=\Phi-\frac{T_j^{\alpha,\mathbf{r}^*}(\Phi)}{T_0} \pmod 1, \tag{5}$$

where $j$ is selected to be sufficiently large that transients in determining the phase resetting curve have dissipated.

Now consider the effects of periodic $\delta$ function stimulation with period $t_s$. Suppose that stimulus $i$ is applied at phase $\Phi_i$. The stimulus shifts the phase to $g(\Phi_i)$ at the end of the stimulus. After an additional time $(t_s)$, a second stimulus is delivered. Then, provided the limit cycle is rapidly reestablished following the stimulus, and the stimulus does not change the properties of the nonlinear equation [18–20],

$$\Phi_{i+1}=g(\Phi_i)+\frac{t_s}{T_0} \pmod 1. \tag{6}$$

Starting from any given initial phase $\Phi_0$, we can iterate Eq. (6). Stable fixed points and cycles correspond to entrainment to the periodic forcing.

Since resetting curves due to stimuli delivered at a single location but measured at two different probes are related by a horizontal shift equal to the phase lag of activation between the two during the underlying rhythm, Eq. (4), the phase transition curves measured at two different locations from a stimulus at a single source are identical under a change in the coordinate system corresponding to an arbitrary choice of phase. Consequently, all fixed points and cycles in Eq. (6) will be preserved under a transformation in the coordinate system. *Therefore, when the phase transition curve is used to make predictions about the periodicity and stability of the dynamics under periodic stimulation, the results will not depend on the location of the measuring probe.*

Previous studies predicted the effects of periodic stimulation in a spatially homogeneous oscillating system [19] and a circulating pulse in a ring of excitable medium [20] based on the phase transition curves. Here we show that, as the stimulus probe is moved away from the circuit determining the period of the oscillation, the predictions of entrainment based on the resetting data may no longer be accurate.

### D. Propagating waves

Periodic stimulation of reentrant waves circulating around an anatomical barrier leads to an entrainment and capture of the reentrant waves if the stimulation period is shorter than the period of the rotation, but longer than the refractory period of the medium. The propagating waves collide with the reentrant waves, so that eventually local points throughout the medium oscillate with the same frequency as the imposed rhythm [5,25]. This earlier work did not explicitly consider the phase of the stimulus.

Suppose that periodic stimuli with a period of $t_s$ are delivered at a location $\mathbf{r}_1$. Assume that a probe at location $\mathbf{r}_2$ measures periodic activation with the same period as the stimulation. The phases of the stimuli delivered at $\mathbf{r}_1$ are measured relative to the time of activation at $\mathbf{r}_2$. During the tachycardia, following stimulus $i$ delivered at $\mathbf{r}_1$ at time $t_i$, call $t_c$ the conduction time for the stimulus to travel from $\mathbf{r}_1$ to $\mathbf{r}_2$. Then the phase of the stimulus measured at $\mathbf{r}_2$ is

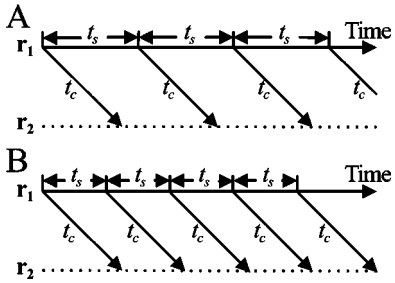


FIG. 2. Schematic diagram of the conduction of an impulse that is delivered at $\mathbf{r}_1$ and that propagates to $\mathbf{r}_2$. The conduction time is $t_c$ and the interstimulus time is $t_s$. (a) When $t_s>t_c$ the phase of the stimulus as measured at $\mathbf{r}_2$ is given by Eq. (7) with $n=1$. (b) When $2t_s>t_c>t_s$ the phase of the stimulus as measured at $\mathbf{r}_2$ is given by Eq. (7) with $n=2$.

$$\phi(\mathbf{r}_2,t_i)=\frac{nt_s-t_c}{T_0} \pmod 1, \tag{7}$$

where $n$ is a constant integer. The value of $n$ depends upon the conduction time between $\mathbf{r}_1$ and $\mathbf{r}_2$ and the stimulation period $t_s$. If the stimulation period is $t_s>t_c$, then $n=1$. If $t_s<t_c<2t_s$, then $n=2$, and so forth. The further the recording site $\mathbf{r}_2$ is from the stimulation site $\mathbf{r}_1$, the greater the value of $n$. The value of $n$ could be computed by determining the rate of change of $\phi(\mathbf{r}_2,t)$ as $t_s$ varies [30]. Figure 2 illustrates the results for two different values of $t_s$. Even if activations at $\mathbf{r}_2$ have the same period as the period of the stimulus at $\mathbf{r}_1$, this does not necessarily reflect entrainment of the reentrant wave by the stimulation. For example, the stimulation at $\mathbf{r}_1$ could completely fail to entrain the tachycardia, but nevertheless there could be complete synchronization with the probe at $\mathbf{r}_2$. This could occur if $\mathbf{r}_2$ was located physically close to $\mathbf{r}_1$, but both sites were comparatively remote from the location of the reentrant circuit.

## III. A SIMPLE CONDUCTION MODEL

In this section we describe a highly simplified model to illustrate resetting and entrainment of reentrant waves that captures some of the basic properties of more realistic models.

In the simple theoretical model we assume that a wave circulates on a one-dimensional ring to which a ''tail'' has been added, Fig. 3. The basic cycle length $T_0$ is given by

$$T_0=\frac{L}{c}$$

where $L$ is the circumference of the ring and $c$ is the velocity of propagation. At any point on the ring, for a time interval of $R$ after passage of the wave, the tissue is refractory. Oth-

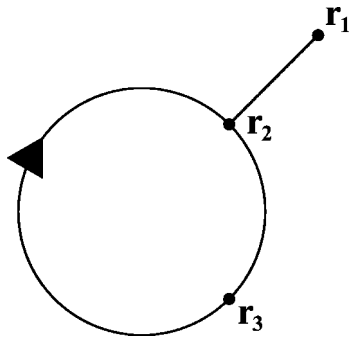


FIG. 3. The simple conduction model. The excitation travels at a fixed velocity around the ring and along the tail.

erwise, the medium is excitable. A stimulus delivered during the refractory period has no effect, whereas a stimulus delivered during the excitable period will generate waves propagating into the excitable medium. The stimulus and the recording sites are not necessarily the same and either or both could be on the tail.

First assume that the stimulus and recording site are identical and that both are directly on the ring at $r_2$ as shown in Fig. 3. We select this point as the fiducial point so that the circulating wave crosses the fiducial point at time $t_0$. The global phase is $\Phi(t)=(t-t_0)/T_0$ (mod 1). The ring is parametrized by an angular coordinate $\theta$. We set $\theta=0$ at the fiducial point so that the angular position of the wave around the ring at time $t$ is $\theta(t)=\Phi(t)$. This example has been set up so that the location of the wave on the ring is the same as the global phase.

If the stimulus is delivered during the refractory period then it has no effect. If the stimulus is delivered outside the refractory time then it will induce two waves, one traveling in the opposite direction to (antidromic) and the other in the same direction as (orthodromic) the original wave. The antidromic wave will collide with the original wave and be annihilated, whereas the orthodromic wave will continue to propagate, leading to a resetting of the original rhythm. The perturbed cycle length $T_k^{r_2,\tau_2}(\Phi(t))$ is

$$\frac{T_k^{r_2,r_2}(\Phi(t))}{T_0}=\begin{cases} k-[1-\Phi(t)], & 1>\Phi(t)>\dfrac{R}{T_0}, \\ k, & \dfrac{R}{T_0}>\Phi(t)>0. \end{cases} \tag{8}$$

Using Eq. (5) we obtain the phase transition curve

$$g(\Phi(t))=\begin{cases} 0, & 1>\Phi(t)>\dfrac{R}{T_0}, \\ \Phi(t), & \dfrac{R}{T_0}>\Phi(t)>0. \end{cases} \tag{9}$$

The time interval during which the stimulus resets the rhythm is called the *excitable gap*. The excitable gap is $G=T_0-R$.

Iteration of Eq. (6) is easily carried out. Provided the stimulation period falls in the range $R<t_s<T_0$, there is a stable fixed point on the period-1 map associated with entrainment of the reentrant excitation to the periodic stimulation. The phase of the fixed point is $t_s/T_0$. This result corresponds to the result obtained using Eq. (7) assuming stimulation and recording in the same locus so that $t_c=0$.

Now consider the effects of periodic stimulation from a site on the ring, e.g., $\mathbf{r}_2$ in Fig. 3, but carrying out the measurements of the phase from a distant site also on the ring, e.g., $\mathbf{r}_3$ in Fig. 3, where the propagation time from the stimulus site to the measuring site is $t_c$. For this case we find

$$g(\phi(t))=\begin{cases} 1-\dfrac{t_c}{T_0}, & 1>\phi(t)>\dfrac{R}{T_0}+\dfrac{t_c}{T_0} \quad \text{and} \quad \dfrac{t_c}{T_0}>\phi(t)>0, \\ \phi(t) & \text{otherwise.} \end{cases} \tag{10}$$

There is a stable period-1 fixed point at $\phi^*=(t_s-t_c)/T_0$ (mod 1) for $t_s>R$. However, if $R<t_c$ this result is not always correct. To illustrate, we assume that $t_c/T_0=1/3$ and that $R/T_0=1/8$. These parameter values are chosen so that multiple waves can be present on the annulus simultaneously and they do not necessarily correspond to physiologically realistic values. In Fig. 4, we show the predicted phase of the stimulus during the entrainment as a function of $t_s/T_0$ using Eqs. (6) and (10) (solid line) compared with the result obtained using Eq. (7) (dashed line). The two results overlap for $t_s>t_c$. Equation (7) gives the correct result for $t_s>R$. The failure of Eq. (6) arises from the difficulty of determining which of the waves measured at $r_3$ is associated with a given stimulus. When there are multiple waves on the ring simultaneously, the necessary operational definition of the phase of the stimulus may lead to an erroneous result from the basic theory.

Now consider the effect of stimulating the excitation from a point $r_1$ off the ring that lies at a distance $l$ from the fiducial point $r_2$ on the ring and on the same radius as $r_2$ (see Fig. 3). Because the conduction from the reentrant pathway can collide with the excitation from the stimulating electrode before it resets the reentrant excitation, the range of phases over which resetting is observed is reduced. The perturbed cycle length is

$$\frac{T_k^{r_1,r_2}(\Phi(t))}{T_0}=\begin{cases} k-1+\Phi(t)+\dfrac{l}{cT_0}, & 1-\dfrac{1}{cT_0}>\Phi(t)>\dfrac{R}{T_0}+\dfrac{l}{cT_0}, \\ k & \text{otherwise}, \end{cases} \tag{11}$$

and the associated resetting curve becomes

$$g(\Phi(t))=\begin{cases} 1-\dfrac{l}{cT_0}, & 1-\dfrac{l}{cT_0}>\Phi(t)>\dfrac{R}{T_0}+\dfrac{l}{cT_0}, \\ \Phi(t) & \text{otherwise}. \end{cases} \tag{12}$$

The range of values over which resetting occurs due to a single pulse decreases as the distance of the stimulus from the ring increases. Specifically, the excitable gap is $(T_0-R-2l/c)$. From this it follows that for $l>c(T_0-R)/2$ there is no resetting. If the phase transition curve is used to predict the effects of periodic stimulation, then one theoretically predicts that there will be 1:1 entrainment for stimulation periods in the range $T_0>t_s>R+2l/c$. However, this is not correct, and in this case the resetting curve can no longer be used to predict the effects of periodic stimulation. The reason for this is that the collisions between the wave from the stimulus and the reentrant wave lead to a reduced range of values for the resetting. During periodic stimulation at a rate $t_s$ in the range $T_0>t_s>R$, the collisions between the waves originating from the periodic stimulation and the reentrant wave will occur successively closer to the reentrant circuit, and the waves originating from the periodic forcing will eventually penetrate the reentrant circuit and entrain the reentrant wave [5,25]. Therefore, the theoretical prediction of the entrainment zone based on the resetting curve will underestimate the range of values leading to entrainment by a value of $2l/c$ for $l<c(T_0-R)/2$. Thus, one can estimate the distance of a stimulus from the reentrant circuit by multiplying the discrepancy between the predicted and observed high frequency boundaries of the 1:1 locking by the velocity of propagation of the wave, provided the stimulus is not very distant from the reentrant circuit.

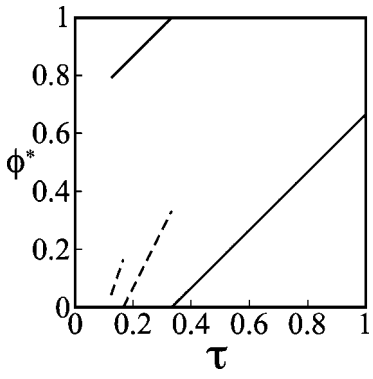


FIG. 4. Predicted value of the fixed point during periodic stimulation from point $r_2$ and recording at point $r_3$ in Fig. 3, where $t_c/T_0=1/3$ and $R/T_0=1/8$. The solid line is obtained using Eqs. (6) and (10) and the dashed line is obtained using Eq. (7). The two results overlap for $t_s>t_c$. $\tau=t_s/T_0$.

## IV. FITZHUGH-NAGUMO EQUATION

We now consider the effects of single and periodic stimulation of the FitzHugh-Nagumo equation, a nonlinear partial differential equation model that has been used as a prototypic model for excitable media. We implemented the following modified version:

$$\frac{\partial v}{\partial t}=\frac{l}{\epsilon}(v-\tfrac{1}{3}v^3-w)+D\nabla^2 v+I_{\text{sitm}}(t)+I_{\text{hold}},$$

$$\frac{\partial w}{\partial t}=\epsilon(v+\beta-\gamma w)R(v), \tag{13}$$

$$R(v)=\frac{0.8}{1.0+10e^{10(v-0.1)}}+0.2,$$

where $v$ is associated with the membrane potential, $w$ is associated with the recovery of the membrane potential, and we assume $\beta=0.7$, $\gamma=0.8$, $\epsilon=0.3$, and $D=1\ \text{cm}^2/\text{sec}$. $I_{\text{stim}}(t)$ is a spatiotemporal current injected into the FitzHugh-Nagumo equation. The sigmoidal function $R(v)$ controls the action potential duration. The equations are solved using the Euler integration scheme with $\Delta t=0.05$ msec and $\Delta r=0.025$ cm in a lattice of $109\times109$ grid points representing an area $2.73\times2.73\ \text{cm}^2$. We generate a central region that is not excitable by assuming $I_{\text{hold}}=-2.5$ in a central circular area of diameter 20 grid points representing a circle of 0.5 cm. No-flux boundary conditions are applied at the edges of the square domain. The excitable region is thus an annular region with an inner boundary composed of a central inexcitable region, and the outer boundary formed by the edges of the square in which the simulations are carried out. In runs in which stimuli are delivered, we set $I_{\text{stim}}=20.0$ at a single grid point with a duration of 2.5 msec or 50 time steps.

Figure 5 illustrates a reentrant wave propagating in the annular domain found by integrating Eq. (13). After a transient, the intrinsic period of the reentrant wave is $T_0=58.3$ msec. The conduction velocity $c$ and the refractory period $R$ of this model are estimated from a plane wave propagating in a homogeneous sheet of the same dimension. The conduction velocity is $c=0.039$ cm/ms and the refractory period is $R=12.1$ msec.

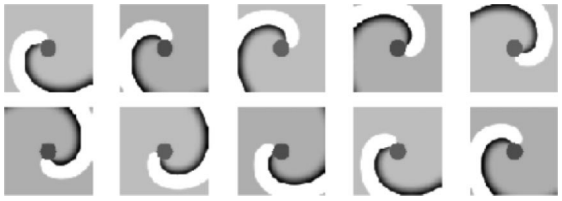

FIG. 5. Numerically integrated reentrant wave in an annulus in the modified FitzHugh-Nagumo equation (13). $T_0=58.3$ ms. The conduction velocity and the refractory period are estimated from propagation of a plane wave in a two-dimensional sheet. The conduction velocity is $c=0.039$ cm/ms and the refractory period is $R=12.1$ ms. In this and subsequent figures, the frames are 7.25 ms apart.

### A. Resetting curve

In this section we determine the resetting curve obtained by stimulating at one location, and recording the resetting at both the stimulation site and a different site.

Figure 6(a) illustrates the effects of stimulation at site $\mathbf{r}_1$ indicated by an asterisk $*$ that is 0.625 cm away from the central inexcitable region. A second site $\mathbf{r}_2$ indicated by a cross is a distance 0.2 cm away from the central inexcitable region. Figures 6(b) and 6(c) show the resetting curves measured from $\mathbf{r}_1$ and $\mathbf{r}_2$, respectively. The time of activation at $\mathbf{r}_1$ precedes the time of activation at $\mathbf{r}_2$ by 15.7 msec. Thus the resetting curves measured at the two sites are related by Eq. (2) with a phase shift of $\phi(\mathbf{r}_1)-\phi(\mathbf{r}_2)=-0.27$.

If the discontinuity in Figs. 6(b) and 6(c) is probed by trying to deliver stimuli that are very close to the phase of the discontinuity, then stimuli are discovered that lead to the initiation of a dynamics in which there are two counterrotating spiral waves in addition to the circulating spiral wave. This result is expected based on earlier analyses. First,

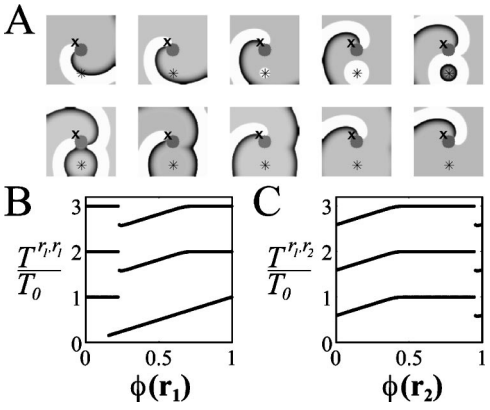


FIG. 6. Resetting of reentrant wave. (a) The stimulus delivered at $\mathbf{r}_1$,*, propagates to the annulus and generates two waves that propagate around the annulus. The antidromic wave collides with the original reentrant wave and drifts away from the sheet. The orthodromic wave becomes a new reentrant wave whose timing has been reset by the stimulus. (b) Perturbed cycle length arising from stimulating at $\mathbf{r}_1$ and recording at $\mathbf{r}_1$. (c) Perturbed cycle length arising from stimulating at $\mathbf{r}_1$ and recording at $\mathbf{r}_2$, $\times$. The perturbed cycle length curves are identical under a shift of $\phi(\mathbf{r}_1)-\phi(\mathbf{r}_2)=-0.27$.

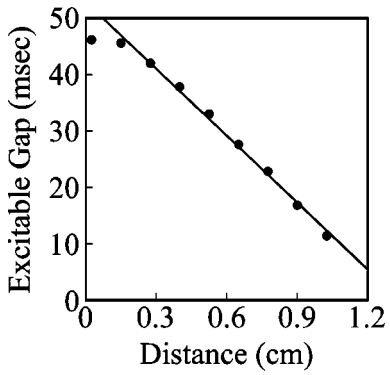


FIG. 7. The excitable gap as a function of the distance from the edge of the central inexcitable region numerically computed in the modified FitzHugh-Nagumo equation. A stimulus delivered from a site that is more than 1.35 cm away from the central inexcitable region does not reset the rhythm.

a ''vulnerable period'' for initiating spiral pairs in models of excitable media is well known [28]. Further, discontinuities in resetting curves of an oscillation imply that stimuli should exist that lead to a different dynamics lying outside the basin of attraction of the oscillation [23].

As the distance from the stimulus to the central inexcitable region is increased, the stimulus resets the reentrant wave over a smaller range of time intervals due to the collision between the wave generated by the stimulus and the reentrant wave. Figure 7 illustrates the decrease of the excitable gap as the distance from the stimulation site to the inexcitable region increases. If the location of the stimulus is less than 0.1 cm away from the central region, the resetting is approximately the same as if the reentrant wave were circulating around a one-dimensional ring with diameter 0.5 cm. In this case, all stimuli reset the wave except those falling in the refractory period of the reentrant wave. If the stimulus is located more than $l=1.35$ cm away from the inexcitable region, none of the stimuli reset the reentrant wave. The size of the excitable gap decreases as $\approx 1.6l/c$ for $1.35>l>0.2$ cm.

### B. Entrainment of reentrant waves

In this section we investigate the entrainment of reentrant waves by periodic stimulation and compare the results with iteration of the phase transition curve. Periodic stimulation is delivered at $\mathbf{r}_1$ and the entrainment results are recorded from $\mathbf{r}_1$ and $\mathbf{r}_2$. For all trials, we apply the initial stimulus 27.4 msec after a reentrant wave passes $\mathbf{r}_1$. Figure 8(a) illustrates the entrainment of the reentrant wave at $\mathbf{r}_1$ with $t_s=47.5$ msec, so that $t_s/T_0=0.82$. The stimulus from $\mathbf{r}_1$ propagates to the inexcitable region. The antidromic wave annihilates the original reentrant wave. The orthodromic wave establishes a new reentrant wave propagating around the annulus. Thus, the periodic stimulation entrains the reentrant wave. When the stimulation is terminated after ten stimuli, the original reentrant wave is reestablished with the same amplitude and frequency as before the stimulation. The time series recorded from $\mathbf{r}_1$ and $\mathbf{r}_2$ during the periodic stimulation are shown in Figs. 8(b) and 8(c), respectively.

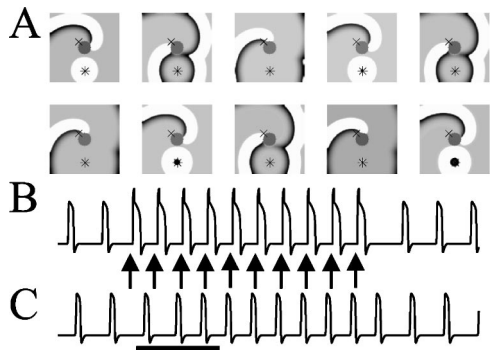


FIG. 8. Entrainment of the reentrant wave in Eq. (13). Periodic stimuli are delivered from $\mathbf{r}_1$ with $t_s/T_0=0.81$, $t_s=47.5$ msec. (a) The first stimulus is applied at 27.4 msec after the last reentrant wave passes $\mathbf{r}_1$. The reentrant wave is entrained after three stimuli. (b) and (c) are the time series trace records from $\mathbf{r}_1$ and $\mathbf{r}_2$, respectively. The arrows in (b) denote the stimuli applied at $\mathbf{r}_1$. The horizontal bar in (c) corresponds to the time interval displayed in (a).

The arrows in Fig. 8(b) indicate the times of the stimulation at $\mathbf{r}_1$. The time interval spanned by animation in Fig. 8(a) is indicated by the horizontal bar under Fig. 8(c).

In order to predict the effects of periodic stimulation constructed from data collected at $\mathbf{r}_2$, the resetting curve from Fig. 6(c) is fitted by a piecewise linear function, and is used to construct a phase transition curve like Eq. (5),

$$g(\phi(\mathbf{r}_2))=\begin{cases}0.41, & 0\leqslant\phi(\mathbf{r}_2)<0.41,\\ \phi(\mathbf{r}_2), & 0.41\leqslant\phi(\mathbf{r}_2)<0.96,\\ 0.41, & 0.96\leqslant\phi(\mathbf{r}_2)<1.\end{cases} \tag{14}$$

Figure 9(a) shows the iteration of the phase transition curve with $t_s/T_0=0.82$. After two iterations $\phi_n$ converges to the fixed point $\phi^*=0.23$. Figure 9(b) represents the entrainment with $t_s/T_0=0.64$. The trajectory approaches the fixed point $\phi^*=0.05$ after two iterations. Figure 9(c) shows the iteration of the phase transition curve for $t_s/T_0=0.47$. There is a stable period-2 orbit. However, numerical integration of the FitzHugh-Nagumo model with $t_s/T_0=0.47$ shows 1:1 entrainment with $\phi^*=0.31$.

Thus, the phase transition curve is not able to predict the entrainment when the stimulation is comparatively fast. The stimulation is at a distance from the inexcitable region and

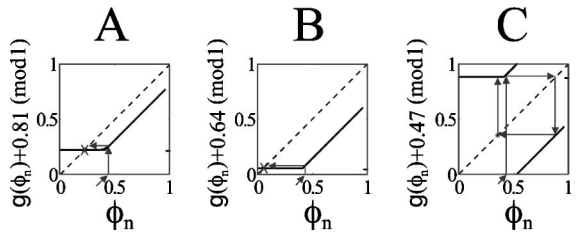


FIG. 9. Iteration of the phase transition curve determined at $\mathbf{r}_2$ with the initial condition of $\phi_0=0.47$. (a) $t_s/T_0=0.81$, $t_s=47.5$ msec. (b) $t_s/T_0=0.64$, $t_s=37.5$ msec. (c) $t_s/T_0=0.47$, $t_s=27.5$ msec. In (c) the trajectory approaches a period-2 orbit even though the numerical simulation of the nonlinear equation gives a stable 1:1 entrainment.

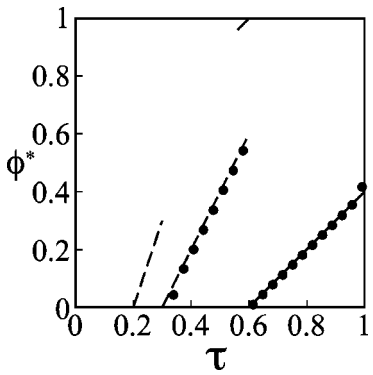


FIG. 10. The entrainment phase as a function of $\tau=t_s/T_0$ using three different methods of computation: iteration of the phase transition curve Eq. (6), solid line; numerical integration of the FitzHugh-Nagumo model, ●; and Eq. (7), dashed line.

this leads to interference between the wave generated from the stimulation and the reentrant wave. Further, the measuring probe is located at a distance from the stimulation and this leads to the simultaneous presence of several waves from the stimulation in the medium, leading to discrepancies in computing the phase of the stimulus (see Fig. 2 and the related discussion). Figure 10 compares the predictions of the location of the fixed point $\phi^*$ as a function of $t_s/T_0$ from the phase transition function (solid line), from Eq. (7) (dashed line), and from numerical simulation of the FitzHugh-Nagumo model (points). In the current case, all three methods agree for $t_s/T_0>0.6$. However, only Eq. (7) gives the correct answer for $R<t_s<t_c$.

## V. EXPERIMENTAL EXAMPLE

To illustrate the application of these concepts to a concrete system, we consider experimental data from a single experiment carried out in a mongrel dog. We hope to report more complete data elsewhere.

### A. Experimental procedures

We used a surgical procedure in which a Y-shaped lesion is made in the right atrium (one of the heart chambers) of a dog [31]. This experimental system supports a circulating excitation that models a human arrhythmia called atrial flutter in which an excitation travels in a circuitous pathway in the right atrium.

Four sites were recorded from both sides of the lesion, Fig. 11. First the flutter was induced by rapid stimulation of the right atrium. Figure 11 shows a recording during flutter. The sharp spikes reflect the activation of the local electrodes. Following induction of the flutter, two different protocols were carried out. In one protocol, single stimuli were introduced every eight cycles to study the resetting of the tachycardia by single pulses. Stimuli were delivered over a range of phases to scan the effects of the stimuli at the different phases of the flutter cycle. Resetting stimuli were delivered from two different locations. In a second protocol, periodic stimuli were delivered from the same two locations. The period of the stimuli was reduced from the intrinsic cycle

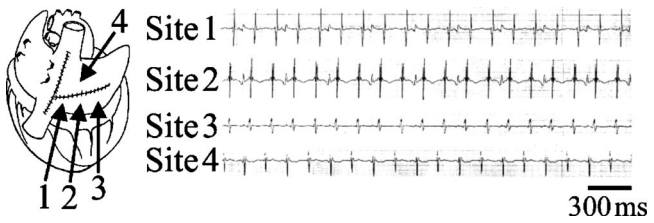


FIG. 11. Schematic diagram of of the experimental preparation carried out in an anesthetized dog. The right atrium of a dog heart is lesioned and sutured in a Y shape following the procedure of [31]. Recordings are carried out from four sites on the right atrium during atrial flutter. The large complexes on each trace, shown in the right hand side of the figure, correspond to the times of activation at each of the sites.

length of the flutter (around 150 msec) to 100 msec in 10 msec decrements.

### B. Resetting curve from different stimulus sites

Stimuli delivered at some of the phases of the flutter reset the flutter. Figure 12(a) shows the effects of a resetting stimulus delivered at site 4, with recordings of the activity from site 2 (upper trace) and site 4 (lower trace).

Figures 12(b) and 12(c) show resetting curves measured from stimuli delivered at site 4 and measured at sites 4 and 2, respectively. The phase shifts between the two sites are $\phi(\mathbf{r}_4)-\phi(\mathbf{r}_2)=0.28$. The resetting curve Fig. 12(c) is fitted with the piecewise linear function

$$\frac{T_2^{\mathbf{r}_4,\mathbf{r}_2}}{T_0}=\begin{cases}2.0, & 0\leqslant\phi(\mathbf{r}_2)<0.26,\\ 1.87, & 0.26\leqslant\phi(\mathbf{r}_2)<0.46,\\ 0.57\phi(\mathbf{r}_2)+1.6, & 0.46\leqslant\phi(\mathbf{r}_2)<0.7,\\ 2, & 0.7\leqslant\phi(\mathbf{r}_2)<1.\end{cases} \tag{15}$$

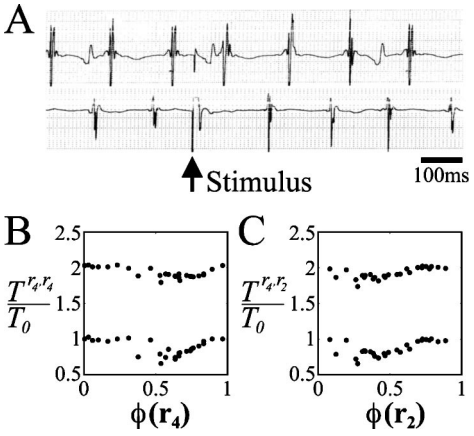


FIG. 12. Resetting curve constructed from the experimental data by stimulating at site 4 in Fig. 11. (a) A stimulus is applied 60 msec after the last excitation at site 4. The upper trace is from site 2 and the lower trace is from site 4. (b) Plot of the perturbed cycle length measured from site 4. (c) Plot of the perturbed cycle length measured from site 2. In both cases the excitable gap is approximately 75 msec. $\Delta\phi=0.5$, and the two resetting curves are related as $\phi(\mathbf{r}_4)-\phi(\mathbf{r}_2)=0.28$.

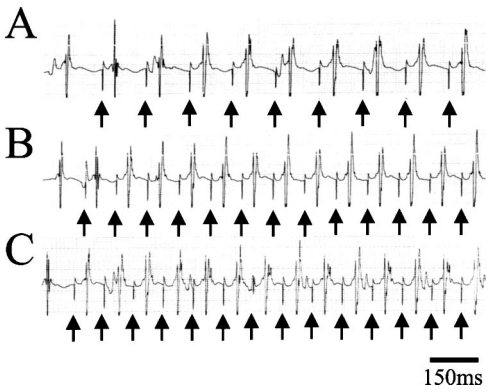


FIG. 13. Experimental studies of the entrainment of atrial flutter with stimulation at site 4 and recording from site 2 in Fig. 11. Bold arrows represent the times of delivery of the stimuli. In each case there is a 1:1 entrainment. (a) $t_s=145$ msec, $t_s/T_0=0.97$; (b) $t_s=130$ msec, $t_s/T_0=0.87$; (c) $t_s=115$ msec, $t_s/T_0=0.77$.

### C. Experimental entrainment of atrial flutter

Figure 13 shows time series traces from the entrainment of atrial flutter induced by stimulating at site 4 at different cycle lengths and recording at site 2. Each bold arrow represents the stimulation applied at site 4. Figure 14 shows the corresponding iterations of the resetting curves based on the resetting curves in Eq. (15). Figures 13(a) and 14(a) correspond to stimulation with $t_s=145$ msec, $t_s/T_0=0.97$, and Figs. 13(b) and 14(b) correspond to stimulation with $t_s=130$ msec, $t_s/T_0=0.87$. In both these cases there is 1:1 entrainment of atrial flutter. However, periodic stimulation with $t_s=115$ msec, $t_s/T_0=0.77$ gives 1:1 entrainment experimentally, Fig. 13(c), but this does not correspond with the results from the iteration of the phase transition curve shown in Fig. 14(c). Figure 15 summarizes the experiment and the theory. The predicted phases of the fixed point during the periodic stimulation from iteration of the phase transition curve (solid line) are compared with the experimentally observed phases (points). At one stimulation frequency, indicated by the triangle in Fig. 15, a different arrhythmia, atrial fibrillation, associated with disorganized propagation in the atria, was induced. Since the maximum shortening of the cycle time by a single stimulus is approximately 20 msec, the

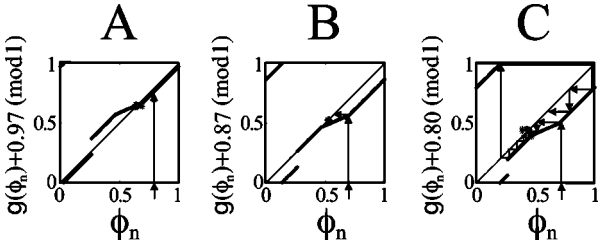


FIG. 14. Iteration of the phase transition curves Eq. (6) for the stimulation parameters shown in Fig. 13. (a) $t_s=145$ msec, $t_s/T_0=0.97$; (b) $t_s=130$ msec, $t_s/T_0=0.87$; (c) $t_s=115$ msec, $t_s/T_0=0.77$. The iteration of the map predicts 1:1 entrainment in (a) and (b), but not in (c). Thus, there is a discrepancy between the iteration of the map and experimental results for the stimulation parameters in (c).

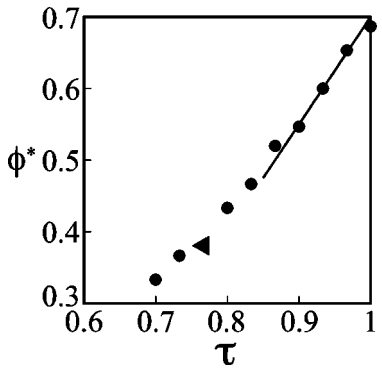


FIG. 15. The phase of the stimulus during stimulation from site 4 and measured at site 2 as a function of $\tau = t_s/T_0$ from the experimental data points and the iteration of Eq. (6) (solid line). The iteration of the map agrees with the data for $1 > t_s/T_0 > 0.87$. However, for $t_s/T_0 < 0.87$, the phase transition map does not predict the 1:1 entrainment that is observed experimentally. In one trial, a different cardiac arrhythmia, atrial fibrillation, was induced, indicated by the triangle.

predicted minimum cycle length for 1:1 entrainment is 130 msec. Thus, although there is good agreement between predicted and observed dynamics for $t_s > 130$ msec, $t_s/T_0 > 0.85$, for smaller values of $t_s/T_0$ the iteration fails to predict the entrainment.

## VI. DISCUSSION

Biological and physical oscillations can usually be affected by suitable stimuli that reset and entrain the rhythms. Previous work demonstrated that iteration of a one-dimensional map based on the resetting induced by single stimuli can be used predict entrainment during periodic stimulation provided the stimuli do not affect the intrinsic properties of the oscillator and the relaxation time to the limit cycle following a stimulus is short compared to the time interval between the periodic stimuli [19,18]. The initial applications were to systems described by limit cycle oscillations in ordinary differential equations. The current work extends these methods to stable oscillations in nonlinear partial differential equations.

Cardiologists often use resetting and entrainment protocols in the clinical study of patients who have serious arrhythmias associated with reentry in an anatomically based pathway [9,11,15,13], often imagined as a one-dimensional ring. An earlier study considered resetting and entrainment of waves circulating on one-dimensional rings [20].

The current work analyzes dynamics of waves circulating in annular domains rather than on one-dimensional rings. In addition we consider situations in which stimuli are delivered at one location and the resetting and entrainment are measured at a second location. This work demonstrates two ways in which the earlier theory breaks down. First, if the stimulus is a distance away from the circuit determining the period of the oscillation, there can be interference between the stimulus and the circulating wave so that the range of phases that lead to resetting is reduced compared to a stimulus directly in the circuit, and the theory fails to predict the entire range of frequencies that lead to entrainment. In theoretical models, the discrepancy between the predicted range of frequencies that lead to 1:1 entrainment and the observed range of frequencies is proportional to the distance of the stimulus from the circuit, provided the stimulus is not too distant from the pathway that defines the reentrant circuit. This observation could be useful in a clinical context to help localize the stimulus relative to a reentrant circuit. A second problem arises when stimulating at one locus and recording at a second locus. If the distance between the stimulating site and the recording site is small, but both these sites are distant from the circuit supporting the reentrant excitation, then entrainment at the recording site does not necessarily reflect the entrainment of the underlying oscillation. If the distance from the stimulating site to the recording is large, then predictions of the phase of the stimulus in the cycle as measured at the recording site may not be correct due to ambiguity of the phase of a given stimulus in measurements at the recording site.

Although the experimental procedures are in principle straightforward, there are practical difficulties encountered when carrying out the experiments. One problem is that a stimulus may sometimes fail to reset the tachycardia, even though stimuli at shorter and longer coupling intervals do reset the tachycardia. The failure may reflect small changes in the efficacy of a stimulus or the excitability of the heart during the tachycardia (the heart is beating during these experiments). The intrinsic noise combined with noise introduced during measurements makes it difficult to fit resetting functions to the experimental data. Moreover, the stimulation can in some instances lead to a change in the rhythm, either by annihilating the rhythm or by inducing atrial fibrillation. These difficulties in the experimental setting would likewise be found in clinical studies. Indeed, although resetting of clinical tachycardias is carried out in some instances [9,14], this is not a usual procedure in the clinic. On the other hand, interpretation of the dynamics during periodic pacing from different sites is proving beneficial to map the anatomical substrate of tachycardias relative to the site of the pacing electrode [13,15–17]. We are not aware of previous quantitative analyses of the connections between resetting and entrainment in the clinical literature.

The current work was carried out with a circular obstacle and a homogeneous medium. If the obstacle is elliptical, the resetting curves are qualitatively similar to what we describe here and once again the size of the excitable gap decreases as the distance away from the inner boundary of the annular region increases. However, if there are heterogeneities that locally increase the refractory period, then the location of the stimulus relative to the heterogeneities and the obstacle(s) may affect the details of the resetting curves [32].

It is not clear whether the current results will be useful in helping physicians to target sites for ablation in patients with reentrant tachycardias. Consider atrial flutter, an arrhythmia associated with a reentrant path similar to the ones considered in the current paper [15,17]. Ablation for atrial flutter is usually successful. In treating atrial flutter, rather than carrying out detailed resetting and entrainment studies, the cardiologist often targets a region of the heart that is believed to

be an ''isthmus'' traversed by the flutter waves. By ablating this isthmus, the flutter pathway is usually eliminated. Further, new clinical mapping techniques are making it possible to visualize the spread of excitation over large regions of the cardiac muscle without carrying out resetting and entrainment [16]. Since carrying out resetting and entrainment protocols is time consuming, this increases the cost of the procedure and also the discomfort to the patient. Finally, as the current paper shows, interpretation of the results of these types of procedures is difficult. In order to lead to practical utility, ways must be developed to streamline the stimulation protocols and to automatically analyze the data in real time.

The current work provides a theoretical foundation for relating resetting and entrainment of reentrant waves. The main motivation arises from cardiology, where reentrant waves in excitable media are an important mechanism underlying serious abnormal cardiac rhythms. We hope that this work provides a stimulus to investigate resetting and entrainment of reentrant waves in other biological and physical systems.

## ACKNOWLEDGMENTS

This research was partially supported by the MRC, CIHR, and FCAR. We thank C. Villemaire for carrying out the experiments. Y.N. thanks the Heart and Stroke Foundation of Canada for support.

[1] R. Fitzhugh, in *Biological Engineering*, edited by H. P. Schwan *et al.* (McGraw-Hill, New York, 1969).
[2] J. Rinzel and J. B. Keller, Biophys. J. **13**, 1313 (1973).
[3] J. Rinzel, in *Research Notes in Mathematics. Nonlinear Diffusion*, edited by W. E. Fitzgibbon III and H. R. Walker (Pitman, London, 1977), pp. 186–212.
[4] J. P. Keener, SIAM (Soc. Ind. Appl. Math.) J. Appl. Math. **39**, 528 (1980).
[5] V. I. Krinsky and K. I. Agladze, Physica D **8**, 50 (1983).
[6] Z. Noszticzius, W. Horthemke, W. D. McCormick, H. L. Swinney, and W. Y. Tam, Nature (London) **329**, 619 (1987).
[7] M. E. Josephson, *Clinical Cardiac Electrophysiology: Techniques and Interpretation*, 2nd ed. (Lea & Febiger, Philadelphia, 1993).
[8] G. R. Mines, J. Physiol. (London) **46**, 349 (1913).
[9] M. E. Josephson *et al.*, in *Tachycardia: Mechanisms and Management*, edited by M. E. Josephson and H. J. J. Wellens (Futura, Mount Kisco, NY, 1993), pp. 505–536.
[10] L. H. Frame and M. B. Simson, Circulation **78**, 1277 (1988).
[11] W. G. Stevenson *et al.*, J. Am. Coll. Cardiol. **11**, 522 (1988).
[12] R. C. Bernstein and L. H. Frame, Circulation **81**, 267 (1994).
[13] W. G. Stevenson *et al.*, J. Am. Coll. Cardiol. **29**, 1180 (1997).
[14] D. J. Callans, D. Schwartzman, C. D. Gottlieb, S. M. Dillon, and F. E. Marchlinski, J. Am. Coll. Cardiol. **30**, 1793 (1997).
[15] A. L. Waldo, J. Cardiovasc. Electrophysiol. **8**, 337 (1997).
[16] W. G. Stevenson, E. Delacretaz, P. L. Friedman, and K. E. Ellison, PACE **21**, 1448 (1998).
[17] D. C. Shah, M. Haissaguerre, P. Jais, A. Takahashi, and J. Clementy, PACE **22**, 344 (1999).
[18] M. R. Guevara and L. Glass, J. Math. Biol. **14**, 1 (1982).
[19] M. R. Guevara, L. Glass, and A. Shrier, Science **214**, 1350 (1981).
[20] T. Nomura and L. Glass, Phys. Rev. E **53**, 6353 (1996).
[21] V. I. Krinsky, V. N. Biktashev, and A. M. Pertsov, Ann. N.Y. Acad. Sci. **591**, 232 (1990).
[22] Y. Rudy, J. Cardiovasc. Electrophysiol. **6**, 294 (1995).
[23] L. Glass and M. E. Josephson, Phys. Rev. Lett. **75**, 2059 (1995).
[24] K. Hall and L. Glass, Phys. Rev. Lett. **82**, 5164 (1999).
[25] V. N. Biktashev, in *Computational Biology of the Heart*, edited by A. V. Panfilov and A. V. Holden (Wiley, Chichester, 1997), pp. 155–170.
[26] In the current context, which involves partial differential equations, $x$ represents the variables describing the excitation wave defined in space. In the previous work concerning oscillations in ordinary differential equations, $x$ represented the value of the variables in the traditional state space of the differential equation.
[27] J. Guckenheimer, J. Math. Biol. **1**, 259 (1975).
[28] M. Kawato and R. Suzuki, Biol. Cybern. **30**, 241 (1978); M. Kawato, J. Math. Biol. **12**, 13 (1980).
[29] A. T. Winfree, *The Geometry of Biological Time*, 2nd ed. (Springer-Verlag, New York, 2001).
[30] This observation shows that measurement of the phase of arrival of a signal at a receiver relative to the time of its transmission from a source could be used to measure the distance between the source and the receiver if the conduction velocity of the intervening medium is known and if the frequency of transmission at the source can be modulated.
[31] L. H. Frame, R. L. Page, and B. F. Hoffman, Circ. Res. **58**, 495 (1986); P. A. Boyden, L. H. Frame, and B. F. Hoffman, Circulation **79**, 406 (1989). The dogs were anesthetized with morphine and $\alpha$-chloralose and mechanically ventilated. Nadolol was used to block cardiac $\beta$-adrenergic receptors and atropine was used to block muscarinic receptors. A programmable stimulator was used to deliver 2 msec pulses of current to reset and capture the atria during the course of the flutter (4–5 mA).
[32] S. Sinha and D. J. Christini, e-print nlin.CD/0107070.